

Design of a robust LQG Compensator for an Electric Power Steering

Marcus Irmer*, Hermann Henrichfreise*

*Cologne Laboratory of Mechatronics, Cologne University of Applied Sciences,
 Cologne, 50679, Germany (e-mail: marcus.irmer@th-koeln.de, hermann.henrichfreise@th-koeln.de)

Abstract: The control of the driver's hand torque of an electric power steering system has been state of the art for years. However, due to nonlinear spring characteristics, gear ratios, and degrees of freedom which are unconsidered in the design model for the controller or observer design, the challenge still lies in the robust implementation of this control approach. In this paper, the results of a systematic model and system analysis are used to develop an approach that solves the current stability and robustness problems existing in the serial development of steering systems while maintaining the same control quality. For this, a modified optimal control design is applied which uses an augmented design model.

Keywords: Mechatronic systems, vehicle dynamic systems, parameter-varying systems, modeling, model reduction, optimal control theory, robust controller synthesis, robustness analysis

1. INTRODUCTION

This paper presents an approach to control the driver's steering torque for electromechanical power steering (EPS) systems based on an invention of Niessen and Henrichfreise (2002). One control approach was published by Henrichfreise et al. (2003) and Graßmann et al. (2003). In the referenced papers, a simplified linear plant model for the steering system with two degrees of freedom (DOF) is used for the controller resp. observer design. It only considers the elasticity of the torsion bar. All other elements are assumed to be rigid. The two degrees of freedom are the angle φ_S of the steering wheel and the angle of the lower steering column, which is equal to the angle φ_P of the pinion. Bröcker (2006), Chen and Chen (2006), and El-Shaer et al. (2009) use a similar design model with the same two degrees of freedom, whereas Chitu et al. (2013) developed a design model with three degrees of freedom where additionally the EPS motor is elastically coupled to the rest of the steering mechanism. Thus, the third degree of freedom is the angle φ_M of the EPS motor. Even in more complex vehicle simulation environments, as in the simulation tool suite ASM from dSPACE (2017), only models with these three degrees of freedom are used.

However, such design models lead to control systems which have a low robustness, since a real steering mechanism contains additional elasticities and degrees of freedom. These elasticities as well as nonlinear plant characteristics are considered in a detailed model of the steering mechanism, which has been validated in many steering applications performed in our workgroup. Based on this nonlinear detailed model, a new design model for the controller and observer design is developed which yields a robust control system. The detailed model is shown in section 2. It contains all relevant elasticities and nonlinear characteristics that may exist in a real steering mechanism. The following section 3 describes the controller and observer design, and in section 4 the corresponding closed-loop system is analysed with respect to both

its dynamic behaviour and its robustness. Finally, a summary is given in section 5.

The investigations are done based on a steering mechanism with an EPS motor in a so-called axially parallel configuration. The methods presented in the following sections can also be applied to other configurations or systems.

2. DETAILED MODEL OF STEERING MECHANISM

Applying the design models from previous publications, our experience with real steering systems showed that these models do not consider all relevant eigenmodes of a steering mechanism. Therefore, a more detailed model of the steering mechanism has been developed. Fig. 1 depicts its physical substitute model with eight degrees of freedom. The individual rigid bodies are labelled with the indices S (steering), P (pinion), R (rack), N (nut), M (motor), C (casing), V (vehicle), WL (left wheel), and WR (right wheel).

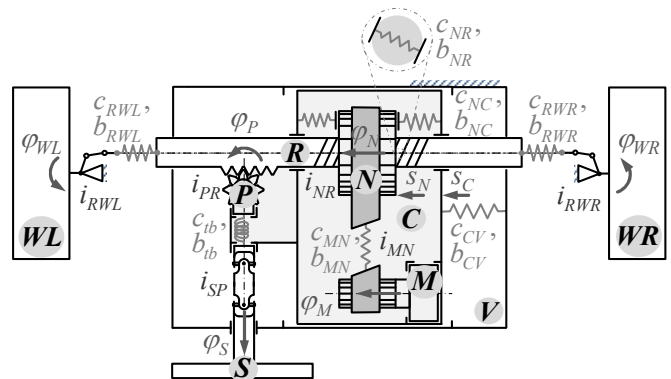


Fig. 1. Physical substitute model of the steering mechanism with eight degrees of freedom

The arrows in Fig. 1 indicate the degrees of freedom. Here, the rack has no degree of freedom. Its deflection s_R depends

on the angle φ_p of the pinion via the gear ratio i_{PR} of the coupling between pinion and rack that is assumed to be rigid. Moreover, it is defined that the rack is located in front of the steering axle in the x -direction of the vehicle coordinate system. Consequently, the pinion gear must be placed behind the rack. This configuration has the advantage that all degrees of freedom and dependent deflections act in positive coordinate directions of the vehicle coordinate system. Furthermore, it is assumed that the pinion bearing is rigidly coupled to the casing and that the casing cannot rotate relative to the vehicle. In addition, there are universal joints in the steering column which have nonlinear gear ratios. Also, the mechanism consisting of tie rod and lever between rack and both wheels has a nonlinear gear ratio i_{RWL} resp. i_{RWR} .

Besides these nonlinear gear ratios, nonlinear spring characteristics were also integrated in the detailed model of the steering mechanism. They are depicted in Fig. 1 by the stiffness c_{NR} of the ball screw drive, stiffness c_{MN} of the belt drive, stiffness c_{NC} of the axial nut bearing, stiffness c_{CV} of the casing attachment, stiffness c_{RWL} resp. c_{RWR} of the attachment of the left resp. right wheel, and the stiffness c_{tb} of the torsion bar (torque sensor). All springs except the spring of the torsion bar have a nonlinear characteristic. Aside from that, additional nonlinear characteristics, such as load-dependent friction and mechanical boundaries, as well as viscosity for each elastic component (viscoelastic component) have been considered in the detailed model. The equations of motion of this nonlinear model have been derived, linearized, and converted into state space representation. Based on this model with eight degrees of freedom, further simplified models can be generated by model order reduction.

Each of these different models for the steering mechanism is extended by a simplified, linear model of a current-controlled EPS motor in form of a first order lag system. Combined, they form the plant model. The plant model consisting of the current-controlled EPS motor and the linearized detailed model of the steering mechanism with eight degrees of freedom will be called “8DOF” in the subsequent sections. It will be used as a model of the real steering system.

A analysis of the model “8DOF” is carried out by Wittler et al. (2017) and Irmer et al. (2019). The papers show that the lowest and therefore most dominant eigenfrequency of the steering system depends not only on the stiffness c_{tb} of the torsion bar but also on the stiffness c_{NR} of the ball screw drive and the stiffness c_{NC} of the axial nut bearing. Hence, a model with two degrees of freedom from Henrichfreise et al. (2003), Bröcker (2006), Chen and Chen (2006), El-Shaer et al. (2009), or others which only considers the stiffness c_{tb} of the torsion bar, does not exactly map this lowest eigenfrequency of the real steering system, whereas other dominant eigenfrequencies are not modelled at all.

The second lowest eigenfrequency depends, inter alia, on the parameters of the viscoelastic wheel attachments. The corresponding eigenmode is characterized by in-phase angular displacements φ_{WL} and φ_{WR} of the wheels. Thus, the viscoelastic wheel attachments must be considered in a plant model that should reflect the second dominant eigenfrequency of the real steering system as well. This is also outlined by Badawy

et al. (1999), Pfeffer and Harrer (2013), and Schramm et al. (2017). Consequently, the models with three degrees of freedom from Chitu et al. (2013), dSPACE (2017), or others also do not sufficiently model the real steering system. Although the models have a higher order, they do not map the second lowest eigenfrequency of the real steering system correctly because they neglect the viscoelastic wheel attachments. Hence, the aforementioned models with two or three degrees of freedom are not suitable for a robust control design. Therefore, the subject of the next chapter is to derive a more appropriate model that will be used for a new control design.

3. CONTROL DESIGN

Fig. 2 shows the block diagram of the closed-loop system consisting of the detailed plant model “8DOF” and the dynamic linear-quadratic-Gaussian (LQG) compensator. The compensator contains the linear optimal static state space controller (LQR) and the linear optimal state space observer (LQE). Their design is the subject of the current chapter.

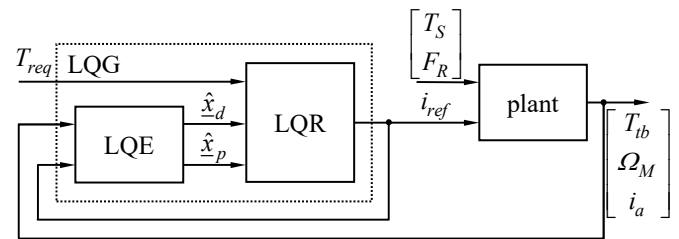


Fig. 2. Block diagram of the closed-loop system with dynamic LQG compensator

For a constant angle φ_s of the steering wheel, the torsion bar torque T_{ib} is equal to the steering torque T_S induced by the driver at the steering wheel. Hence, the task of the compensator is to adjust the torsion bar torque T_{ib} to a given externally generated requested steering torque T_{req} . By setting the requested steering torque T_{req} as the reference variable, it is possible to generate a defined steering feel for the driver with an additional outer control loop. The steering torque T_S itself and the rack force F_R , which results from the contact between the tire and the road as well as from the friction at the rack, represent disturbance variables for the control system. The effect of these disturbance variables is compensated by a disturbance feedforward. Since it is not possible to measure all state and disturbance variables, an optimal observer is used to provide an estimate \hat{x}_p of the state vector x_p of the plant and an estimate $\hat{x}_d = [\hat{T}_S, \hat{F}_R]^T$ of the disturbance input vector $[T_S, F_R]^T$ of the plant. For this, the observer uses measurements of the torsion bar torque T_{ib} , motor angular velocity Ω_M , and motor current i_a , as well as the reference current i_{ref} for the inner control loop of the EPS motor (Graßmann et al. (2003), Henrichfreise et al. (2003)).

The control system must satisfy the requirements of a good control and disturbance behaviour as well as it must have a higher degree of robustness against unconsidered eigenmodes and parameter uncertainties in the plant model than the control systems of previous approaches. A precondition for a good dynamic behaviour is active vibration damping of the

oscillating modes of the mechanical system. Therefore, an LQG compensator is designed based on Henrichfreise (1997) which considers the natural limitations of the real system, so that no bounds are exceeded during normal operation. However, the use of a high-order model for the compensator (controller and observer) design causes problems because its parameters often cannot be identified or vary substantially during operation. For example, the eigenfrequencies change under load due to the nonlinear spring characteristics and gear ratios. This is detrimental to the control, since it does not match the respective eigenmodes of the plant model sufficiently. Consequently, a compensator of the lowest possible order should always be implemented. Nevertheless, the design model should not be reduced too much.

Thus, a method is described in the following section that can be applied to reduce the detailed model without impairing its characteristics, so that the resulting reduced model can be used for the subsequent compensator design. The method preserves stability and provides a high approximation quality in the relevant frequency range for the control. Starting point is the state space representation

$$\begin{aligned}\dot{\underline{x}} &= \underline{A}\underline{x} + \underline{B}\underline{u} \\ \underline{y} &= \underline{C}\underline{x} + \underline{D}\underline{u}\end{aligned}\quad (1)$$

of the stable linearized detailed model of the steering mechanism with the (n) -vector \underline{x} of the state variables of the steering mechanism and $n = 16$ (eight degrees of freedom). The aim is to determine a well-suited reduced model

$$\begin{aligned}\dot{\underline{x}}_{red} &= \underline{A}_{red}\underline{x}_{red} + \underline{B}_{red}\underline{u} \\ \underline{y}_{red} &= \underline{C}_{red}\underline{x}_{red} + \underline{D}_{red}\underline{u} \approx \underline{y}\end{aligned}\quad (2)$$

of the steering mechanism with a (m) -vector \underline{x}_{red} and $m < n$ for the design of a robust control.

3.1 Design Model based on Modal Order Reduction

Reduced models can be generated in different ways, for example by physically motivated order reduction (Wittler et al. (2017)). However, the control systems resulting from this reduced design models are not necessarily robust against the unconsidered eigenmodes of the plant model. Therefore, this paper will present an alternative approach based on modal order reduction. For this purpose, the detailed model of the steering mechanism from (1) is transformed into modal form

$$\begin{aligned}\dot{\underline{z}} &= \underline{A}\underline{z} + \underline{B}\underline{u} \\ \underline{y} &= \underline{C}\underline{z} + \underline{D}\underline{u}\end{aligned}\quad (3)$$

with $\underline{z} = [\underline{z}_1, \underline{z}_2]^T$, $\underline{A} = \text{diag}(\underline{A}_1, \underline{A}_2)$, $\underline{B} = [\underline{B}_1, \underline{B}_2]^T$, and $\underline{C} = [\underline{C}_1, \underline{C}_2]$, where \underline{z}_1 describes the state vector of the dominant state variables and \underline{z}_2 the state vector of the residual state variables of the steering mechanism. Since all eigenvalues of the linearized detailed model of the steering mechanism are different, the corresponding system matrix \underline{A} can be diagonalized, so that the submatrices $\underline{A}_1 = \text{diag}(\lambda_1, \dots, \lambda_m)$ and $\underline{A}_2 = \text{diag}(\lambda_{m+1}, \dots, \lambda_n)$ of the modal system matrix \underline{A} become diagonal.

The corresponding transfer matrix of the linearized detailed model of the steering mechanism follows from the equation

$$\begin{aligned}\underline{G}(s) &= \underline{C}(s\underline{I} - \underline{A})^{-1}\underline{B} + \underline{D} \\ &= \frac{\underline{C}_1 \text{adj}(s\underline{I} - \underline{A}_1)\underline{B}_1 + \underline{D} \det(s\underline{I} - \underline{A}_1)}{\det(s\underline{I} - \underline{A}_1)} \\ &\quad + \frac{\underline{C}_2 \text{adj}(s\underline{I} - \underline{A}_2)\underline{B}_2}{\det(s\underline{I} - \underline{A}_2)}.\end{aligned}\quad (4)$$

If only the state vector \underline{z}_1 of the dominant state variables of the steering mechanism is considered, the state space representation of the modal reduced model of the steering mechanism becomes

$$\begin{aligned}\dot{\underline{z}}_1 &= \underline{A}_1\underline{z}_1 + \underline{B}_1\underline{u} \\ \underline{y}_{red} &= \underline{C}_1\underline{z}_1 + \underline{D}\underline{u}.\end{aligned}\quad (5)$$

This reduced model has the same dominant eigenvalues $\lambda_1, \dots, \lambda_m$ as the detailed model. However, the zeros of the individual transfer paths can be different.

The corresponding transfer matrix of the reduced model is

$$\begin{aligned}\underline{G}_{red}(s) &= \underline{C}_1(s\underline{I} - \underline{A}_1)^{-1}\underline{B}_1 + \underline{D} \\ &= \frac{\underline{C}_1 \text{adj}(s\underline{I} - \underline{A}_1)\underline{B}_1 + \underline{D} \det(s\underline{I} - \underline{A}_1)}{\det(s\underline{I} - \underline{A}_1)}.\end{aligned}\quad (6)$$

Comparing this equation with (4) yields that the transfer matrix $\underline{G}(s)$ of the detailed model can be partitioned into the transfer matrix $\underline{G}_{red}(s)$ of the modal reduced model and a transfer matrix $\underline{G}_{residual}(s)$ for the residual part

$$\underline{G}(s) = \underline{G}_{red}(s) + \underline{G}_{residual}(s).\quad (7)$$

Assuming the transfer matrix $\underline{G}(s)$ does not contain any integral behaviour or this has been neglected, the stationary gains of the individual transfer paths of the linearized detailed model of the steering mechanism results from the equation

$$\begin{aligned}\lim_{s \rightarrow 0} \underline{G}(s) &= \lim_{s \rightarrow 0} \underline{G}_{red}(s) + \lim_{s \rightarrow 0} \underline{G}_{residual}(s) \\ &= \underline{G}_{red}(0) + \underline{G}_{residual}(0).\end{aligned}\quad (8)$$

For the general case $\underline{G}_{residual}(0) \neq \underline{0}$ this means that the modal order reduction cannot reproduce the stationary gains of the detailed model. Nevertheless, the stationary error can be eliminated by an adaptation of the feedthrough matrix

$$\underline{D} = \underline{D} + \underline{G}_{residual}(0).\quad (9)$$

This implies that the transfer behaviour of the residual eigenmodes of the plant model is assumed to be sufficiently fast that it can be considered proportional. Thus, the final state space representation of the modal reduced model of the steering mechanism becomes

$$\begin{aligned}\dot{\underline{z}}_1 &= \underline{A}_1\underline{z}_1 + \underline{B}_1\underline{u} \\ \underline{y}_{red} &= \underline{C}_1\underline{z}_1 + \underline{D}\underline{u}.\end{aligned}\quad (10)$$

The reduced plant model consisting of the modal reduced model of the steering mechanism with $m = 6$, which corresponds to a model with three degrees of freedom, and the current-controlled EPS motor is henceforth denoted by “3DOF modal”.

By neglecting the residual state variables of the steering mechanism in (5) and the adaptation of the feedthrough matrix in (9), additional zeros may occur in the individual transfer paths. Here, a zero is created in the right s-half plane in the control transfer path from the control variable i_{ref} to the controlled variable T_{ib} of the reduced plant model “3DOF modal”. However, this zero is located so far to the right that its effect is only evident in the high-frequency range far above the bandwidth of the control. This is visible in the corresponding frequency response of the control transfer path shown in Fig. 3. The same holds for the other transfer paths.

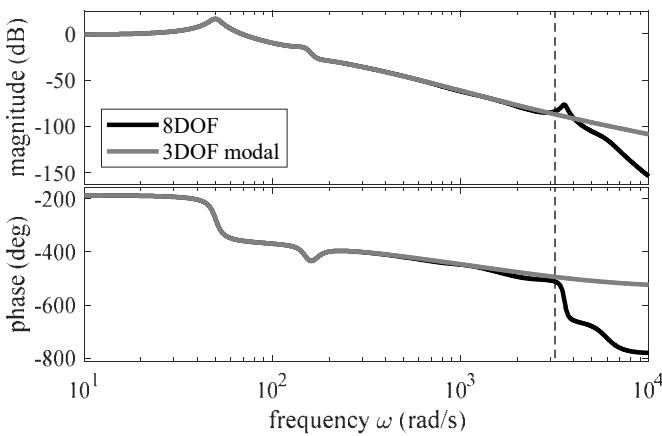


Fig. 3. Frequency response of the control transfer path of the detailed and the reduced plant model

Additionally, Fig. 3 illustrates the frequency response of the control transfer path of the detailed plant model “8DOF”. It can be seen that the frequency response of the reduced plant model “3DOF modal” matches the frequency response of the detailed plant model “8DOF” with sufficient accuracy up to frequencies greater than 3000 rad/s. Since the reduced plant model “3DOF modal” based on (10) has the same dominant eigenvalues and the same steady-state gains as the detailed plant model “8DOF”, the step responses of the individual transfer paths of both models are also almost identical. Therefore, this reduced plant model is a suitable approximation of the detailed plant model. It is the starting point for the following LQR and LQE design.

3.2 LQR Design

The subsequent section describes the design of the optimal static state space controller using the reduced plant model “3DOF modal” under the assumption that all its state variables and disturbance variables are measurable. For this, the reduced plant model is augmented by suitable linear models for reference and disturbance excitation and a weighting model (Henrichfreise (1997)). However, a calculation of the feedforward gains as shown by Henrichfreise (1997) does not

provide steady-state accuracy for this application. The reason for this is that for both reference and disturbance excitation, the steady state requires a control variable i_{ref} unequal to zero. Since the LQR design not only minimizes the control error $e = T_{req} - T_{ib}$ but also minimizes the use of the control variable i_{ref} , steady-state accuracy cannot be achieved. Therefore, an alternative calculation of the reference and disturbance feedforward gains is developed.

First, the reference feedforward gain k_r is calculated according to the block diagram of the closed-loop system shown in Fig. 4.

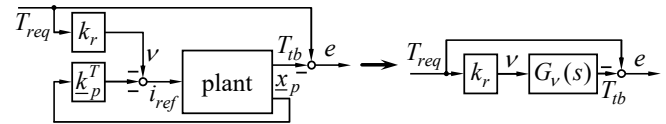


Fig. 4. Block diagram of the closed-loop system with reference feedforward

Based on the reduced plant model, the transfer function $G_v(s)$ of the controlled system with state vector feedback can be determined. Then, the error transfer function is

$$G_e(s) = 1 - k_r G_v(s) \quad (11)$$

If now steady-state accuracy is requested for at least step-shaped reference excitation, the constant gain factor for the reference feedforward must be

$$k_r = 1 / G_v(0) \quad (12)$$

The gains for the disturbance feedforward can be calculated similarly. For this, Fig. 5 shows the block diagram of the controlled system with disturbance feedforward.

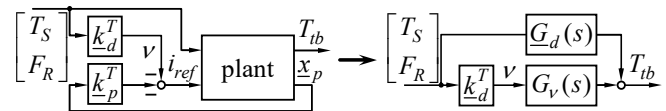


Fig. 5. Block diagram of the closed-loop system with disturbance feedforward

For the transfer matrix from the disturbance input vector $[T_S, F_R]^T$ of the plant to the torsion bar torque T_{ib} , the equation

$$\underline{G}_z(s) = \underline{G}_d(s) + \underline{k}_d^T G_v(s) \quad (13)$$

is given, where $\underline{G}_d(s)$ is the transfer matrix of the controlled system for the disturbance input vector and $G_v(s)$ the transfer function of the aforementioned controlled system with state vector feedback. If here steady-state accuracy also is requested for at least step-shaped disturbance excitation, the equation

$$\underline{k}_d^T = \underline{N}_d(0) / \underline{N}_v(0) \quad (14)$$

follows for the disturbance feedforward, where $\underline{N}_d(s)$ describes the numerator polynomial matrix of the transfer ma-

trix $\underline{G}_d(s)$ and $N_v(s)$ the numerator polynomial of the transfer function $G_v(s)$.

3.3 LQE Design

After the controller gains have been determined in the LQR design, an optimal state space observer is inserted into the control system that provides optimal estimates for the state and disturbance variables of the plant, since these are often not measurable as assumed in the LQR design. Starting point for the design of the linear observer is again the reduced plant model “3DOF modal”. This model is augmented by a suitable disturbance model for the realization of a disturbance observation and a stochastic environment (Henrichfreise (1997)). The minimization of the observer estimation error $\underline{x} - \hat{\underline{x}}$ for the augmented model with $\underline{x} = [\underline{x}_p, T_S, F_R]^T$ provides the values of the optimal observer gain matrix. Thereby, a higher robustness of the control system can be achieved by aspiring loop transfer recovery (LTR) with appropriate process noise intensities in the LQE design (Henrichfreise (1997)).

4. SYSTEM ANALYSIS

The behaviour of the control system is first analysed using linear models in the time and frequency domain. The closed-loop system consists of the detailed plant model “8DOF”, which describes the real plant with adequate accuracy, and a compensator designed with the previously described reduced model “3DOF modal”. In contrast, the aforementioned papers only use a simple plant model for system analysis. Such an approach does not allow to analyse how robust the control system is against the eigenmodes of the real steering mechanism that are unconsidered in the design model. Thus, the plant model used for system analysis should always be as detailed as possible.

4.1 Dynamic Behaviour of the Control System

Fig. 6 depicts the reference step response and the disturbance step responses of the closed-loop system for a requested steering torque T_{req} of 1 Nm, an actual steering torque T_S of 1 Nm, and a rack force F_R of 1 kN. The individual settling times of the step responses as well as the overshoots resp. amplitudes of the controlled variable T_{tb} are sufficiently small. Furthermore, the control approach ensures steady-state accuracy in the case of step-shaped reference or disturbance excitation. Hence, the dynamic behaviour of the control system is good.

The slow decay of the control errors results from a transmission zero which is unfavourably located in the plant model. A more detailed system analysis is carried out for a related design model by Imer et al. (2019).

4.2 Robustness of the Control System

In this section, the robustness of the control system will be analysed. The robustness characteristics can be derived from the Nyquist plot of the open-loop system which is created by cutting the closed-loop system from Fig. 2 at the control in-

put i_{ref} of the plant model. For the given system with only one control variable i_{ref} , the gain margin and the phase margin can be used to assess the robustness of the control system.

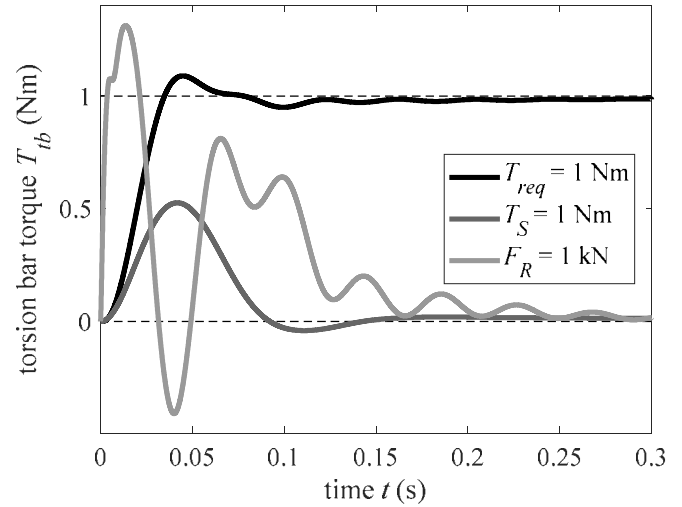


Fig. 6. Step responses of the closed-loop system

Fig. 7 depicts the Nyquist plots of the open-loop system consisting of the detailed plant model “8DOF” and the LQG compensator designed with the reduced model “3DOF modal”. In the plant model, the moments of inertia J_{WL} and J_{WR} of the wheels, all stiffnesses c_{NR} , c_{NC} , c_{CV} , c_{RWL} , and c_{RWR} , as well as the values of the gear ratios i_{RWL} and i_{RWR} between rack and wheels are varied, while the compensator is always designed with unchanged and constant design model parameters. The Nyquist plots illustrate that the control system is stable for all tested parameter variations and that the robustness is always satisfactory. All systems have an almost infinite gain margin and a phase margin of at least 40° . Thus, a design model which has been modally reduced in this way provides excellent robustness characteristics.

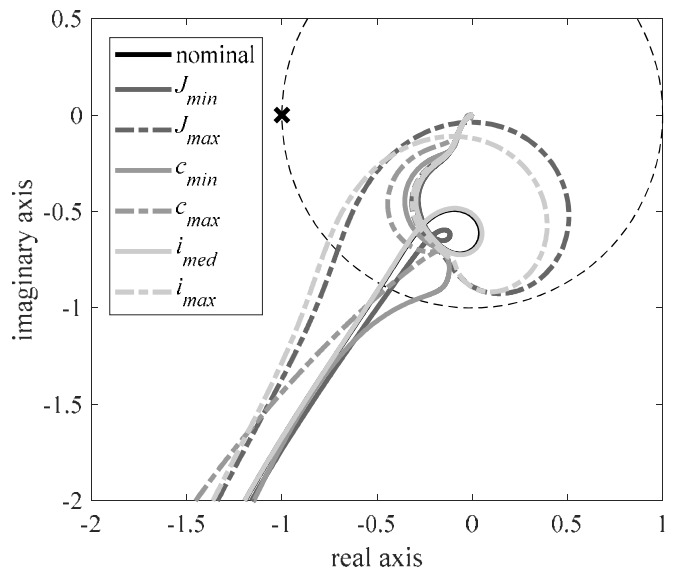


Fig. 7. Nyquist plots of the open-loop system with parameter variations in the plant model

Even for a combined load-dependent variation of the stiffnesses in the plant model – for example, because of an instantaneous operating point characterized by a specific steering torque as well as external forces and torques acting on the tires – the robustness characteristics of the control system are good. In the case of a higher steering torque and nonlinear spring characteristics in the real steering system, this leads to increased stiffnesses for the springs in the linearized plant model, which is displayed in Fig. 7 for a large steering torque with the corresponding curve c_{max} . In this way, the nonlinear characteristics of the steering system are taken into account in the analysis with linear models. In addition, the curve c_{min} describes an operating point where the stiffnesses of the plant are smaller than assumed in the compensator design due to fatigue or inaccurate parameter identification.

The curve J_{min} resp. J_{max} illustrates the result for the case that the moments of inertia J_{WL} and J_{WR} of the wheels in the plant model are minimal ($J_{WL} = J_{WR} = 0.8 \text{ kg}\cdot\text{m}^2$) resp. maximal ($J_{WL} = J_{WR} = 1.7 \text{ kg}\cdot\text{m}^2$), and the curve i_{med} resp. i_{max} for the case that the rack is slightly ($s_R = 0.013 \text{ m}$, $\rightarrow i_{RWL} = 0.17 \text{ m/rad}$, $i_{RWR} = 0.16 \text{ m/rad}$) resp. maximally ($s_R = 0.08 \text{ m} \rightarrow i_{RWL} = 0.15 \text{ m/rad}$, $i_{RWR} = 0.11 \text{ m/rad}$) deflected. A deflection s_R of the rack results in different values for the gear ratios i_{RWL} and i_{RWR} of the right and left wheel attachment due to the kinematics of the tie rod and lever linkages. Despite these parameter variations, the control system remains stable, whereas a control system containing a compensator which has been designed with a model that does not consider the viscoelastic wheel attachments would become unstable.

The parameter changes described here are a selection of the parameter variations conducted for the plant model. All corresponding control systems with unchanged parameters for the compensator designed with the reduced model “3DOF modal” show comparably good robustness characteristics. Therefore, these results are not presented here.

4.3 Simulation Results

In the subsequent chapter, the results of the nonlinear simulation model of the closed-loop system are displayed. The simulation model consists of the nonlinear detailed plant model with eight degrees of freedom and the compensator designed with the reduced plant model “3DOF modal”. In addition to load-dependent friction, nonlinear spring characteristics and gear ratios, as well as mechanical boundaries in the nonlinear plant model, the nonlinear simulation model also contains process noise, measurement noise, and quantization.

The curves presented in Fig. 8 show the simulation results if the nonlinear simulation model is excited from 0.05 s on with a requested steering torque T_{req} of 2 Nm, from 0.4 s on with an actual steering torque T_S of 2 Nm, and from 0.7 s on with constant disturbance torques of 25 Nm at both wheels. The curves indicate that the load-dependent friction is visible in the simulation results. The friction acts against the EPS motor torque and leads to smaller amplitudes of the reference step response compared to the results of the linear closed-loop system from Fig. 6. This can be seen in the upper left dia-

gram of Fig. 8 from 0.05 s on. In addition, the friction has a significant effect on the estimate \hat{F}_R of the disturbance force F_R at the rack, which is displayed in the lower left diagram.

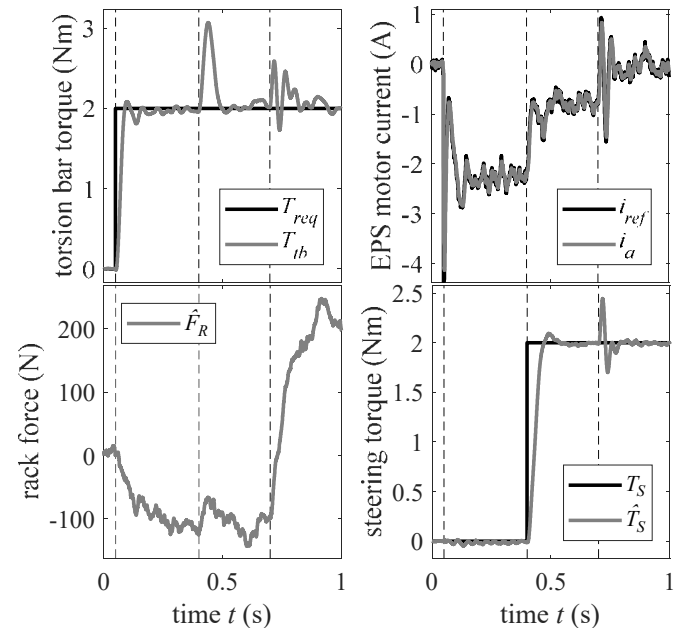


Fig. 8. Time histories of the reference and controlled variable (top left), disturbance variables (bottom), and control variable (top right) of the nonlinear closed-loop system

The disturbance torques at both wheels also affect the estimate \hat{F}_R of the disturbance force F_R at the rack, so that the observer treats these disturbance torques as an equivalent force F_R . The fact that in this experiment the disturbance due to the road contact acts at the wheels as in the real system and not at the rack as assumed in the observer design causes that the springs of the wheel attachments are significantly deformed. The other springs are also deformed, and the rack is deflected, so that the nonlinear spring characteristics and gear ratios also have an influence on the time histories. This can be seen in larger overshoots of the controlled variable T_{ib} and larger amplitudes of the control variable i_{ref} resp. i_a from 0.7 s on compared to the results of the linear closed-loop system from Fig. 6. Nevertheless, the nonlinear closed-loop system remains stable.

Additionally, Fig. 9 shows the results of the same experiment described above if the compensator is designed with a model that does not approximate the viscoelastic wheel attachments. The design model is a model with two degrees of freedom comparable to the model from Henrichfreise et al. (2003), Bröcker (2006), Chen and Chen (2006), or El-Shaer et al. (2009). It will be called “2DOF” in the following. It can be seen that up to 0.7 s the results of the nonlinear closed-loop system containing a compensator designed with the model “2DOF” are similar to the results of the nonlinear closed-loop system containing the compensator designed with the model “3DOF modal”. However, as soon as the closed-loop system is excited from 0.7 s on with a disturbance torque at both wheels due to the road contact, the compensator with the design model “2DOF” becomes unusable, as this compensator

leads to a large and only slowly decaying oscillation of the controlled variable T_{lb} .

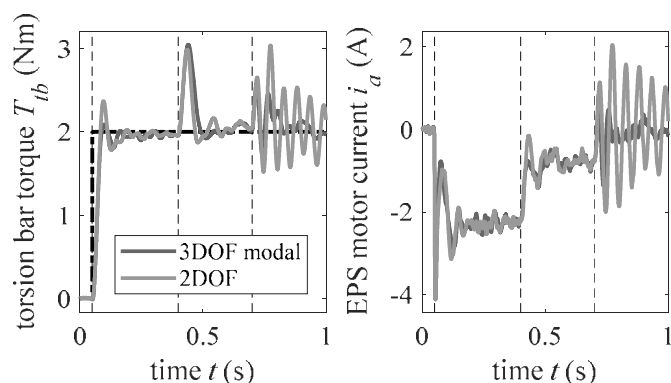


Fig. 9. Time histories of the controlled variable (left) and EPS motor current (right) of the nonlinear closed-loop systems containing compensators designed with different models

A similarly poor dynamic behaviour of the closed-loop system in the case of a disturbance excitation at the wheels due to the road contact is also obtained with a design model with more degrees of freedom if, like the model "2DOF", it does not consider the viscoelastic wheel attachments. Therefore, the design model "3DOF modal" is the optimally reduced model, since it has a minimal order while at the same time it models all dominant eigenmodes of a steering mechanism.

5. CONCLUSION AND OUTLOOK

The paper describes the design of an optimal control for the driver's steering torque of an electromechanical power steering (EPS) system. For this, an LQG compensator consisting of an optimal static state space controller (LQR) with reference and disturbance feedforward control and an optimal state space observer (LQE) with disturbance estimation is used. The LQG compensator provides active vibration damping and disturbance compensation. For the controller and observer design, a model is used that reflects all dominant eigenmodes of a steering mechanism, especially the critical eigenmode due to the viscoelastic wheel attachments. In the above-quoted papers this critical eigenmode was not included in the design models. Therefore, the resulting control systems showed a lack of robustness. In addition, these simple models of the plant were used not only for the control design but also as the plant model for the analysis of the closed-loop system. In this paper, a nonlinear detailed model of the steering mechanism with eight degrees of freedom is used to build the plant model for the analysis. This plant model represents the real steering system much better than the analysis models used in previous publications. Hence, the novelty of this paper lies in this detailed plant model and the method of deriving a reduced model from it.

The resulting closed-loop system shows a good dynamic behaviour and a high robustness against external disturbances, unconsidered degrees of freedom, nonlinear system characteristics, and plant parameter variations. Thus, the presented control fulfils the requirements for a modern steering system and allows the adaptation of the steering feel to the current

driving situation. In the next step, this approach will be applied to steer-by-wire systems.

REFERENCES

- Badawy, A., Zuraski, J., Bolourchi, F., and Chandy, A. (1999). Modeling and Analysis of an Electric Power Steering System. In *SAE 1999 World Congress & Exhibition*. SAE International, Detroit
- Bröcker, M. (2006). New Control Algorithms for Steering Feel Improvements of an Electric Powered Steering System with Belt Drive. In *Vehicle System Dynamics*, volume 44, pages 759-769
- Chen, X. and Chen, X. (2006). Control-Oriented Model for Electric Power Steering System. In *SAE 2006 World Congress & Exhibition*. SAE International, Detroit
- Chitu, C., Lackner, J., Horn, M., Srikanth Pullagura, P., Waser, H., and Kohlböck, M. (2013). Controller design for an electric power steering system based on LQR techniques. In *COMPEL - The international journal for computation and mathematics in electrical and electronic engineering*, volume 32, no. 3, pages 763-775.
- dSPACE (2017). *ASM Vehicle Dynamics Reference*, release 2017-B. dSPACE, Paderborn.
- El-Shaer, A. H., Sugita, S., and Tomizuka, M. (2009). Robust Fixed-Structure Controller Design of Electric Power Steering Systems. In *2009 American Control Conference*. American Automatic Control Council, St. Louis
- Graßmann, O., Henrichfreise, H., Niessen, H., and Hammel, K. v. (2003). Variable Lenkunterstützung für eine elektromechanische Servolenkung. In *23. Tagung „Elektronik im Kraftfahrzeug“*. Haus der Technik, Stuttgart.
- Henrichfreise, H. (1997). Prototyping of a LQG Compensator for a Compliant Positioning System with Friction. In *TransMechatronik*. HNI-Verlagsschriftenreihe, Paderborn.
- Henrichfreise, H., Jusseit, J., and Niessen, H. (2003). Optimale Regelung einer elektromechanischen Servolenkung. In *Fachtagung Mechatronik 2003*. VDI, Fulda.
- Irmer, M., Haßenberg, M., Briese, H., and Henrichfreise, H. (2019). Robust Control of an Electric Power Steering with unconsidered Modes and Parameter Uncertainties. In *10th International Munich Chassis Symposium 2019*. Springer Vieweg, Munich.
- Niessen, H. and Henrichfreise, H. (2002). Vehicle steering system for controlling a steering or steering lock angle for at least one wheel of a vehicle. International patent no. *WO 02/076806 A1*. World Intellectual Property Organization, Geneva.
- Pfeffer, P. and Harrer, M. (2013). *Lenkungs-handbuch – Lenksysteme, Lenkgefühl, Fahrdynamik von Kraftfahrzeugen*. Springer Vieweg, Wiesbaden.
- Schramm, D., Hesse, B., Maas, N., and Unterreiner, M. (2017). *Fahrzeugtechnik – Technische Grundlagen aktueller und zukünftiger Kraftfahrzeuge*. De Gruyter Oldenbourg, Duisburg.
- Wittler, G., Haßenberg, M., Briese, H., Schubert, T., and Henrichfreise, H. (2017). Systematic model based vibration analysis of a controlled electric power steering system. In *8th International Munich Chassis Symposium 2017*. Springer Vieweg, Munich.